The Energy of Interaction between Two Acetone Molecules: A Potential Function Constructed from ab Initio Data

Jose M. Hermida-Ramón* and Miguel A. Ríos

Departamento de Química Física, Facultade de Química, Universidade de Santiago de Compostela, Av. das Ciencias S/N, C.P. 15706, Santiago de Compostela, Spain

Received: October 13, 1997; In Final Form: January 28, 1998

An analytical function representing the energy of interaction in the acetone dimer was constructed on the basis of ab initio (MP2/6-31+G*) calculations for 327 configurations. The inclusion of electron correlation in the ab initio calculations was essential for satisfactory reproduction of experimental data, as was the avoidance of basis set superposition error by means of the counterpoise method. The analytical potential function was fitted to the ab initio data using a weighting scheme favoring good fit in low-energy regions. The minimum of the function, −4.83 kcal/mol, corresponds to a C_{2h} symmetry in which the monomers are antiparallel and are linked by four hydrogen bonds. Three low-energy stationary points corresponding to transition states with differing numbers of hydrogen bonds and energy were also located. The quality of the function was corroborated by inspection of derived isoenergetic contour maps and of its prediction for the temperature dependence of the second virial coefficient. As a further test, a Monte Carlo simulation of liquid acetone was performed in the canonical ensemble, and energetic properties and radial distribution functions were computed.

1. Introduction

Knowledge of intermolecular potentials is necessary for the development of theoretical models that explain the properties of matter and for molecular dynamics (MD) or Monte Carlo (MC) simulation studies.[1] In general, computational limitations impose the need to work with pairwise additive potentials for the energy of interaction of several molecules of the substance or substances being studied. In recent years, analytical potential functions representing this energy have been constructed on the basis of ab initio (*ai*) calculations for numerous pairs of medium-sized molecules, including the dimers of methanol[2] and hydroxylamine[3] and the heterodimers water-butanol,[4] water-methanol,[5] and water-hydroxylamine.[6] Some of these analytical potential functions have been used for liquid-phase simulations. Despite the importance of acetone as a solvent, we know of no *ai*-based potential for acetone−acetone interaction, although the static[7] and dynamic[8,9] properties of acetone have been studied in MD and MC simulations with empirical potentials that do not explicitly take into account the hydrogen atoms.

In this work we constructed a potential that does explicitly include hydrogen atoms (and hence hydrogen bonding) by fitting a suitable analytical expression to the results of *ai* calculations for 327 configurations of the acetone dimer (this correspond to 1308 configurations when symmetry is taken into account). In this context, we also investigated the discrepancy between gas-phase infrared (IR) results,[10] which suggest that the acetone dimer has a C_{2h} structure, and the different predictions of the only previous *ai* study of the acetone dimer.[11] The MC simulations[1] of the pair-potential reveal energetics and structure compatible with experimental results; thus, the simulation seems to show the reliability of using our estimated *ai* pair-potential. We believe that our results may serve to orient studies of intermolecular interactions in larger systems containing carbonyl groups; the only previous *ai*-based intermolecular potential for molecules capable of forming hydrogen bonds involving a carbonyl group has been developed[12] for molecules smaller than acetone (specifically, the water-formaldehyde heterodimer). All *ai* calculations were performed using the GAUSSIAN 94 package.[13] Dimer intermolecular energy was calculated using the supermolecule method.

2. Method

2.1. Computational Level. Because the intermolecular interaction energy was expected to be small (no more than a few kcal/mol) compared with the total energy of a dimer, and hence to require a fairly high computational level for good results, we carried out tests at a variety of levels to arrive at a satisfactory compromise between accuracy and computational effort. To begin with, we optimized the geometry of the acetone monomer both with and without inclusion of electron[14] correlation effects by MP2. We found that even Hartree−Fock (HF) results obtained with a rather large basis set reproduced the experimental[15−18] data less well than MP2 results obtained with much smaller basis sets, underestimating bond lengths and overestimating the dipole moment (Table 1). Double-ζ Dunning/Huzinaga[19] and split valence shell[20] basis sets have been used at the MP2 level. Good MP2 results required the inclusion of both diffuse and polarization functions on the heavy atoms, but little was gained by including them on the hydrogen atoms too.

To compare the basis sets as regards prediction of the interaction energy of the dimer by the "supermolecule" method, calculations were performed with the geometric parameters of the monomer fixed at their experimental values and/or the values corresponding to the minimum-energy structure found with each basis set. In all cases, the dimer configuration with the most negative energy with these fixed monomer geometries afforded C_{2h} structures with four hydrogen bonds of the kind shown in

S1089-5639(97)03309-4 CCC: $15.00
Published on Web 03/24/1998

TABLE 1: Geometry (Å, degree) and Dipole Moment (debyes) of Acetone: Experimental Values and Results at Various Levels

basis set	$r_{(C-O)}$	$r_{(CM-C)}$	$r_{(CM-H)}$[a]	α_{CM-C-O}	α_{H-CM-C}[a]	τ_{HpCMCO}	τ_{HCMCHp}	μ
D95	1.273	1.540	Hp, 1.101 H, 1.106	121.4	Hp, 109.9 H, 110.0	0.0	120.8	3.20
6-31+G	1.267	1.521	Hp, 1.096 H, 1.101	121.3	Hp,109.5 H, 110.3	0.0	121.2	3.33
6-31++G	1.267	1.521	Hp, 1.096 H, 1.101	121.3	Hp, 109.5 H, 110.3	0.0	120.7	3.31
6-31G**	1.186	1.511	Hp, 1.078 H, 1.084	121.6	Hp,109.8 H, 110.1	0.0	121.0	2.57
6-31+G*	1.231	1.512	Hp, 1.091 H, 1.096	121.7	Hp, 109.8 H, 110.1	0.0	121.0	3.14
6-31++G*	1.232	1.512	Hp, 1.091 H, 1.096	121.7	Hp, 109.8 H, 110.1	0.0	121.0	3.13
6-31++G**	1.231	1.512	Hp, 1.086 H, 1.091	121.7	Hp, 109.9 H, 110.0	0.0	121.1	3.07
6-31++G(2d,p)	1.222	1.514	Hp, 1.087 H, 1.092	121.8	Hp, 110.0 H, 110.0	0.0	121.2	3.02
6-31++G(2d,2p)	1.222	1.514	Hp, 1.086 H, 1.092	121.8	H, 110.0 Hp, 110.0	0.0	121.2	2.99
HF/6-311++G (2d,2p)	1.187	1.510	Hp, 1.078 H, 1.084	121.6	Hp, 110.0 H, 110.0	0.0	121.0	3.28
dimer[b], 6-31+G*	1.235	1.508	Hp, 1.092 H, 1.096 Hb, 1.096	121.6	Hp, 109.8 H, 110.7 Hb, 108.9	6.0	H,120.2 Hb, 121.6	3.62
experimental[c]	1.210 ± 0.004	1.517 ± 0.003	1.091 ± 0.003	122.00 ± 0.25	108.5 ± 0.5	0.0	120.0	2.93 ± 0.03
experimental[d]	1.180	1.540	0.985	128.3	102.5	0.0	120.0	

[a] Hp is the hydrogen in the CM·C(O)·CM plane. [b] Geometry of the monomer in the dimer, obtained by full optimization of all coordinates; Hb is the hydrogen-bonding H atom. [c] Values taken from gas-phase microwave rotation spectra;[15] dipole from ref 18. [d] From liquid-phase X-ray scattering.[16,17]

TABLE 2: Interaction Energy (kcal/mol) In An Acetone Dimer With C_{2h} Symmetry (see text) as Calculated at the HF and MP2 Levels Using Various Different Basis Sets, With and Without Avoidance of Basis Set Superposition Error by the Counterpoise (CP) Method (Equation 2)

		D95	6-31G**		6-31+G*		6-31++G*	6-31++G**		6-31++G (2d,2p)		6-31++G(2d,2p)	6-311++G (2d,2p)
method	level	OPT[a]	OPT	EXP[b]	OPT	EXP	EXP	OPT	EXP	OPT	EXP	EXP	OPT
CP	MP2	−4.05	−3.70	−3.89	−4.85	−4.96	−5.00	−4.91	−5.00	−5.39	−5.57	−5.62	
	HF			−2.87		−3.70	−3.71		−3.71		−3.43	−3.48	−3.25
eq 1	MP2	−1.76	−5.13	−6.78	−7.03	−7.11	−7.24	−7.14	−7.19	−5.83	−7.06	−7.02	
	HF			−4.68		−4.14	−4.17		−4.18		−3.09	−3.82	−3.54

[a] OPT: Monomer geometry optimal for the isolated monomer according to the computational level being used. [b] EXP: Monomer geometry obtained from gas-phase microwave rotation spectra.[15]

Figure 4A. Table 2 lists, for a structure approximately at the center of this cluster of optimal configurations, both the uncorrected interaction energies ΔE_{int} calculated using the following formula:

$$E_{int} = E_{AB}(AB) - E_A(A) - E_B(B) \quad (1)$$

(where the arguments in parentheses indicate the basis set being used), and the values obtained using the counterpoise method[21]

$$E_{int} = E_{AB}(AB) - E_A(AB) - E_B(AB) \quad (2)$$

so as to avoid basis set superposition error (BSSE).

All HF results afforded interaction energies smaller in absolute magnitude than the range estimated from experimental data, −4.92 to −4.71 kcal/mol,[11] although the value obtained with the basis set 6-31G** appeared to exhibit the frequently observed mutual near-cancellation of BSSE by the error due to not taking electron correlation into account. The MP2 calculations,[22] as expected, greatly overestimated the interaction energy when split valence shell basis sets[20] and eq 1 were used. The MP2 results obtained with eq 2 show that it is necessary to introduce diffuse functions to obtain good interaction energies. This need might be due to the better representation of wave function at larger internuclear distances. These calculations appear to confirm the results of the study of the monomer in that the most appropriate basis set was again 6-31+G*, which with the monomer geometry it predicted as optimal afforded an interaction energy in the experimentally estimated range. The fact that 6-31+G* performed better than larger basis sets (which appeared to overestimate E_{int} even when eq 2 was used) may have been due to mutual cancellation of errors from multipoles and polarizabilities contributions to the interaction energy. Alternatively, the apparent error in the results of the larger basis sets may reflect inaccuracy on the part of the experimentally based estimate, which was arrived at assuming the unknown values of certain parameters and also involved experimental error in the determination of the enthalpy of formation of the dimer. Be that as it may, the coincidence of the experimental and 6-31+G* estimates, together with the results obtained for the monomer, the rapid increase in computation time with basis set size, and the relatively small difference between the interaction energies obtained with 6-31+G* and the larger basis sets, led us to decide to use MP2/6-31+G* calculations and eq 2 to obtain the sample of ai interaction energies to which the analytical potential would be fitted.

After obtaining the sample of ai interaction energies in accordance with the sampling plan described in the next section, we explored the possibility of going on to optimize intramolecular geometry for each intermolecular configuration in the sample. The lowest interaction energy in the sample, −4.85

TABLE 3: Intermolecular Geometry (Å and Degrees) and Energy (with CP) of Interaction of the Acetone Dimer At or In the Neighborhood of Stationary Points (see Figure 4)[a]

	global min.	inter. min.	sample min.	fit min	inter. T.S. 1	sample T.S. 1	fit T.S. 1	inter. T.S. 2	sample T.S. 2	fit T.S. 2	fit T.S. 3
r_{c1-c5}	3.233	3.195	3.353	3.338	3.864	4.123	4.027	4.863	4.900	4.927	5.929
θ_{O2C1C5}	73.6	75.6	72.6	72.4	84.2	76.0	89.7	57.2	60.8	56.4	0.0
$\varphi_{C5C1O2CM3}$	271.0	270.0	270.0	270.0	270.0	270.0	270.0	0.0	0.0	0.0	0.0
θ_{O6C5C1}	73.6	75.5	72.6	72.4	41.7	46.8	45.7	57.8	58.3	56.4	180.0
$\varphi_{O6C5C1O2}$	180.0	180.0	180.0	180.0	180.0	180.0	180.0	180.0	180.0	0.0	0.0
$\varphi_{CM7C5C1O2}$	59.3	59.2	59.5	59.6	0.0	0.0	0.0	180.0	0.0	180.0	0.0
$E_{(kcal/mol)}$	−5.01	−4.65	−4.85	−4.83	−3.71	−3.41	−3.75	−2.46	−2.47	−2.32	−2.21

[a] As given by MP2/6-31+G* ab initio calculations and the fitted potential function (fit columns). Global: by full optimization of all coordinates. Inter: by optimization of intermolecular coordinates, with intramolecular coordinates fixed at their optimal values for the isolated monomer. Sample: nearest configuration in the sample of ab initio data to which the potential function was fitted.

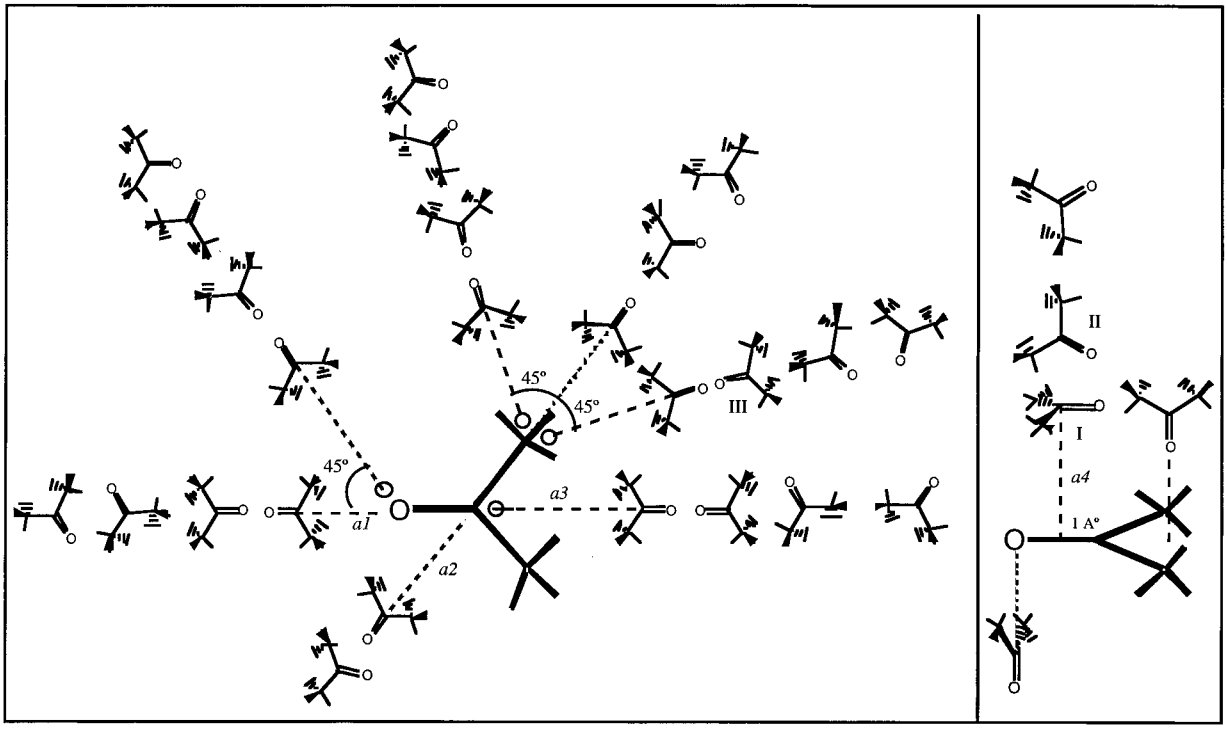

Figure 1. The scheme used to obtain the sample of ab initio data to which the analytical potential function was fitted. Lines starting at small circles lie at 45° to the CM·C(O)·CM plane of the base monomer.

kcal/mol, was 0.16 kcal/mol above that of the configuration obtained by full optimization of the dimer geometry at the MP2/6-31+G* level [see the Sample Min. and Global Min. columns of Table 3, which also shows the corresponding intermolecular geometries; the intramolecular geometry obtained by the full (global) optimization procedure is shown in Table 1 (dimer)]. The energy of the configuration obtained by optimizing intermolecular parameters with intramolecular parameters fixed at the optimal values for the isolated monomer (Inter. Min. column in Table 3) was even further above the value obtained by full optimization (for an explanation of this behavior, see the *Discussion*, Section 3.3, first paragraph). Optimizing the intramolecular geometry with the intermolecular parameters fixed at their Sample Min. values gave an interaction energy that was 0.37 kcal/mol more negative than the Sample Min. value of −5.22 kcal/mol, probably primarily because the rotation of the methyl groups had shortened each of the four hydrogen bonds by 0.2 Å. Eventually, however, it was decided not to optimize intramolecularly for two reasons. First, optimize intramolecularly would greatly prolong calculations. Second, fixing intramolecular geometry gave rise to only rather slight geometric inaccuracy and to an error in the interaction energy that, although larger than for other molecules such as methanol,[2] was still only ∼7% for configurations with four hydrogen bonds and would no doubt be less for those with fewer hydrogen bonds.

2.2. Sampling the Configuration Space. The configuration space of the dimer was sampled with the geometry of the monomers fixed at the optimum given by MP2/6-31+G* calculations for the isolated monomer. The sampling scheme, based on chemical considerations, is shown in Figure 1. Samples were taken with one of the monomers at 10 different distances from the second (base) monomer.

With the intent of reproducing the low-energy region of the energy manifold as faithfully as possible, the 300-point configuration sample already mentioned was subsequently supplemented with a further 30 configurations chosen in the neighborhood of the low-energy stationary points of a provisional analytic potential fitted to the 300-point sample (these 30 configurations include the structure used to obtain the data of Table 2). Three configurations with *ai* energies >50 kcal/mol were eventually removed, leaving a final sample consisting of 327 configurations for each of the four quadrants generated by the two molecular symmetry planes.

2.3. Characteristics of the Potential Function. The function fitted to the ai E_{int} data, E^*_{int}, assumes the pairwise

additivity of contributions by individual atom pairs: where U_{ij},

$$E^*_{int} = \Sigma_{i\in A} \Sigma_{j\in B} U_{ij} \tag{3a}$$

the contribution of the pair formed by atom i on monomer A and atom j on monomer B, depends only on the distance r_{ij} between these two atoms. The U_{ij} values are given by

$$U_{ij} = A_{ij} \exp(-B_{ij} r_{ij}) - C_{ij}/r_{ij}n + D_{ij}/r_{ij} \tag{3b}$$

where the A_{ij} term represents repulsive interactions due to orbital overlap, the B_{ij} and C_{ij} terms jointly represent multipole−charge and multipole−multipole interactions, and the D_{ij} term represents Coulombic charge−charge interaction.

Because the long-range behavior of the potential, which is crucial for its use in simulation studies, is determined almost exclusively by the D_{ij} parameter, these parameters were not among those optimized in fitting eqs 3a and b to the *ai* energy data. Instead these parameters were determined in a chemically more meaningful way as the products q_iq_j of the charges on the corresponding atoms, which were calculated by optimization so as to reproduce the MP2/6-31+G* molecular electrostatic potential under the constraint that the MP2/6-31+G* dipole moment be reproduced exactly. Once the D_{ij} had been determined, the other parameters in eq 3b were obtained by fitting eqs 3a and b to the *ai* interaction energies under the constraint that the A_{ij} and B_{ij} must be positive (which ensured positive energy at close range). The optimization procedure was a Marquardt−Levenberg[23] least-squares algorithm, and good fit in low-energy regions was favored by giving each point s in the sample the weight

$$w(s) = 1 + 100 \exp[(E_{int}(s) - E_{ref})/0.6] \tag{4}$$

where the constant $E_{ref} = -4.85$ kcal/mol is the lowest energy in the *ai* sample.

3. Results

3.1. Ab Initio Data. The sample point with the lowest *ai* interaction energy, −4.85 kcal/mol, belongs to the series of configurations obtained by stepping the "variable" monomer along line *a4* with the antiparallel relative orientation labeled I in Figure 1. In the lowest-energy configuration (one of the extra 30 included in addition to the 300 conforming to the scheme shown in Figure 1), each central carbon lies 3.2 Å from the C═O bond of the other monomer. The particularly low energy of these configurations is attributable to the four hydrogen bonds they allow to be formed, two for each oxygen atom.

There are four other series of low-energy configurations in the sample. In the series of lowest energy, in which three hydrogen bonds can be formed, the variable monomer lies on *a4* with its CM·C(O)·CM plane perpendicular to that of the base monomer and its C═O bond oriented toward the methyl groups of the latter (II in Figure 1). The lowest interaction energy of this series, −3.41 kcal/mol, is attained when the central carbon of the variable monomer is 4.0 Å from the C═O bond of the other.

In another series, in which two hydrogen bonds can be formed, the CM·C(O)·CM structures of the two monomers are coplanar and the CM−C−O angles face each other with the C═O bonds of each oriented toward the methyl group of the other (the second configuration on line *a2* in Figure 1). The lowest interaction energy of this series, −2.47 kcal/mol, is attained when the central carbons are 4.0 Å from each other.

TABLE 4: Point Charges Reproducing the MP2/6-31+G* Molecular Electrostatic Potential and the Molecular Dipole Moment of Acetone and Used to Calculate the D_{ij} of Eq 3b

q_C	q_O	q_{CM}	q_H	μ (D)
0.7963	−0.5513	−0.5510	0.1429	3.14

TABLE 5: Optimized Parameters[a] of the Fitted Function (Equations 3)

		A_{ij}	B_{ij}	C_{ij}
C	C	83899.0850	3.77349729	4136.17162
C	O	2876471.30	5.75901836	−649.741659
C	CM	4431947.96	5.21740647	−151.870846
C	H	5378.27531	4.14951179	−96.9533680
O	O	3226.75032	2.72183801	1164.74169
O	CM	143432.335	3.98846255	−580.429687
O	H	7064.43282	3.91835387	273.819781
CM	CM	3463121.36	5.37122471	−1863.48035
CM	H	3261.84314	3.15515101	438.697631
H	H	425.234032	2.92043030	14.729590

[a] A_{ij} in kcal·mol^{-1}; B_{ij} in Å^{-1}; and C_{ij} in kcal/mol^{-1} Å^4.

Finally, in both the other low-energy series of note, the oxygen of one monomer "attacks" the central carbon of the other along the line bisecting the CM−C−CM angle of the latter, and lowest energy is attained when the O and C atoms are 4.0 Å apart. This lowest interaction energy is −2.45 or −1.97 kcal/mol for dihedral angles of 45 and 0°, respectively between the CM·C(O)·CM planes of the two monomers (i.e., depending on whether the configuration is like the second on line *a3* or the fourth on line *a1* in Figure 1).

3.2. The Potential Function. Of the values tried for the n exponent in eq 3b, $n = 4$ was the one affording the best equilibrium between the fit to the ab initio interaction energies and the representation of the substance properties. Potentials with terms in r_{ij}^{-4} have previously been used by Scheraga and co-workers[24] to model the interaction between water and methylamine or methylammonium ion.

Table 4 lists the q_i used to calculate the D_{ij} of eq 3b, and Table 5 lists the optimized values of the A_{ij}, B_{ij}, and C_{ij}. The data in Table 4 show that the charge of the methyl carbon is almost equal to the oxygen charge; it may seem unusual if the chemical reactivity of the molecule is considered, but this high negative charge may be attributed to the positive charge of the hydrogen atoms. These charges added to the negative charge of the methyl carbon atom give a slightly negative charge for the methyl group, the same behavior appearing in empirical potentials.[7,25] The dipole moment given in Table 4 is ∼7% bigger than the experimental value; however, we considered that this error may be accepted. Whichever the case, it could be useful making use of a slightly overestimated dipole for the pair-potential parametrization so as to allow for the induced dipoles in the liquid-phase simulations.

Figure 2 compares the *ai* interaction energies of <25 kcal/mol (<5 kcal/mol in the inset) with the corresponding values of the fitted potential function (the diagonal lines in these figures merely show what perfect correlation would be like, they are not fitted regression lines). As expected given the weighting function used, agreement improves as interaction energy falls; the most negative energies are very well fitted by the potential function. Importantly, the clustering of the data on either side of the diagonal lines in Figure 2 shows that there is no systematic tendency of the potential to overestimate or underestimate the *ai* data.

Figure 3 compares the fitted potential function with the *ai* data as regards the way in which the interaction energy of the configurations labeled I, II, and III in Figure 1 varies with the

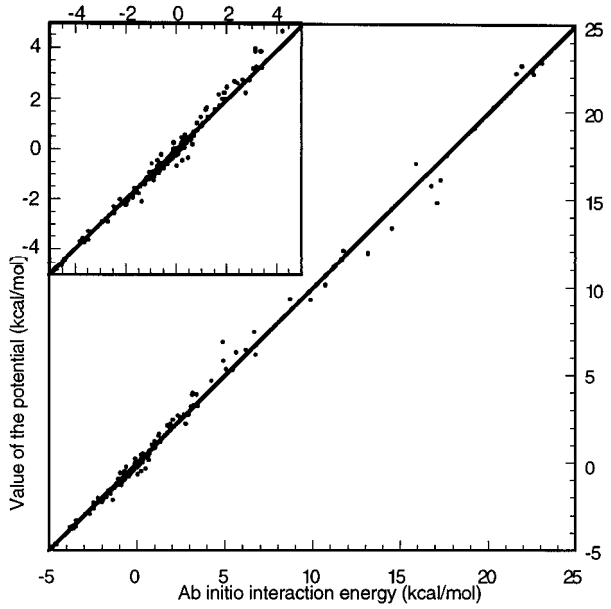

Figure 2. Comparison of the sample of ab initio interaction energies with those given by the fitted potential.

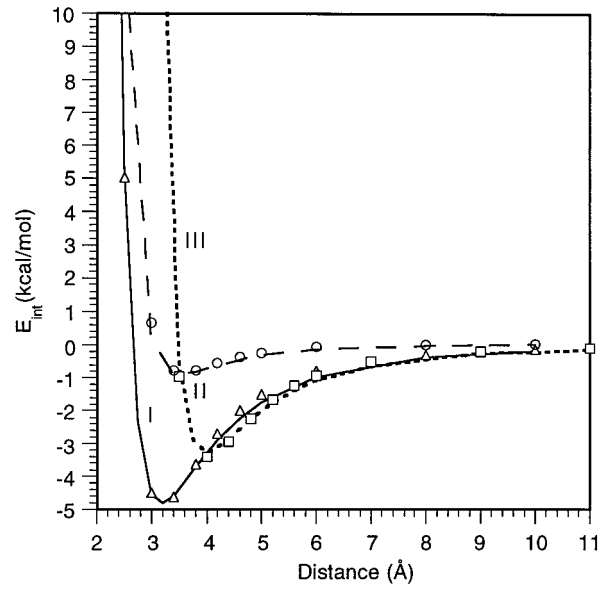

Figure 3. Potential curves for the configurations labeled I, II and III in Figure 1, taken along lines *c2*, *c2*, and *b3*, respectively of that figure, together with corresponding ab initio values of the interaction energy.

distance between the monomers. In the lowest-energy series in the sample (I), the fitted function correctly reproduces the depth of the potential well, but overestimates its width, leading to errors of up to ∼0.3 kcal/mol in the interaction energy on the walls of the well. In the other low-energy series, (II), the reverse occurs: the width of the potential well is well reproduced, but its depth is underestimated by ∼0.1 kcal/mol (although this is not a significant difference given the absolute values of these energies). In the less stable configuration (III), in which the C═O bond of one monomer points directly toward a methyl group of the other, the energy discrepancies are again quite slight. However, as in the other two series, the potential curve is globally smoother than would be required for perfect fit, but the general tendency might be considered as a good fit. Positive *ai* interaction energies are well fitted in all three series.

3.3. Stationary Points. The stationary points of the potential function were detected using the program ORIENT[26] after modification to allow r_{ij}^{-4} terms. Table 3 lists the geometries and potential values of the four most relevant stationary points (Fit columns) together with the geometries and *ai* interaction energies of the nearest configurations in the sample (Sample columns) and those of nearby stationary points of the *ai* dimer energy under variation of only intermolecular parameters (Inter. columns). Note that the latter are not necessarily stationary points of the interaction energy without BSSE under the same constraint because the "ghost" orbitals involved in calculating the $E_\alpha(AB)$ (with α = A or B), of the monomers in eq 2 depend on the geometry of the dimer. This dependence is not taken into account in the *ai* optimization process, which means that the optimization is in a not free BSSE surface. The BSSE changes the value of the interaction energy and can also change the relative order of the interaction energy between two points. For example, the reason the Inter. Min. interaction energy in Table 3, −4.65 kcal/mol, is higher than the Sample Min. value, −4.85 kcal/mol, must be that BSSE is much larger for the Inter Min. dimer geometry than for the Sample Min. dimer geometry and it changes the relative order between both points.

TABLE 6: Intermolecular Vibration Frequencies of the Acetone Dimer in cm^{-1}

HF	MP2	function	experimental[a]
42.7	59.6	35.6	
52.5	71.5	53.5	
62.7	77.5	54.5	
63.2	97.3	55.5	
78.3	104.6	68.6	94.7
141.1	145.6	76.4	125.0

[a] Experimental frequencies from far-IR technique.[10]

The absolute minimum of the fitted potential corresponded to the antiparallel geometry shown in Figure 4A (which also shows the atom numbering scheme used in what follows). This configuration is in keeping with the experimental IR results of Knözinger and Wittenbeck[10] and is similar to one of the conformers − not the most stable − that was predicted by the HF/3-21G and HF/4-31G calculations of Frurip et al.[11] (although Frurip et al. calculated a much longer C1−C5 distance, 3.84 Å, and a much less negative interaction energy, −0.98 kcal/mol). This configuration is very similar to that of lowest interaction energy in the sample, differing by only 0.019 Å in the C1−C5 distance and by only 0.02 kcal/mol in interaction energy.

Table 6 lists harmonic intermolecular vibration frequencies obtained from HF and MP2 *ai* calculations and from the fitted potential function (using ORIENT[26]), together with two experimental frequencies measured by Knözinger and Wittenbeck.[10] These frequency values, the only ones available, refer to the acetone dimer embedded in a cryogenic matrix and therefore they cannot be considered rigorously; however, they can provide quite a useful reference. Overall, the two experimental frequencies are predicted slightly better by MP2 than by HF calculations. The fitted function affords values that are of the right order of magnitude but are too small, especially in the case of the highest frequencies, is undoubtedly because of the excessive smoothness of the fitted potential (see also the previous discussion of Figure 3). The discrepancy with respect to the *ai* values is probably also contributed to by the fact that the latter were calculated directly from dimer energy data, whereas the fitted potential models the interaction energy given by eq 2.

The stationary point of next-to-lowest energy of the fitted potential, a transition state with an energy of −3.75 kcal/mol, is the configuration with three hydrogen bonds shown in Figure

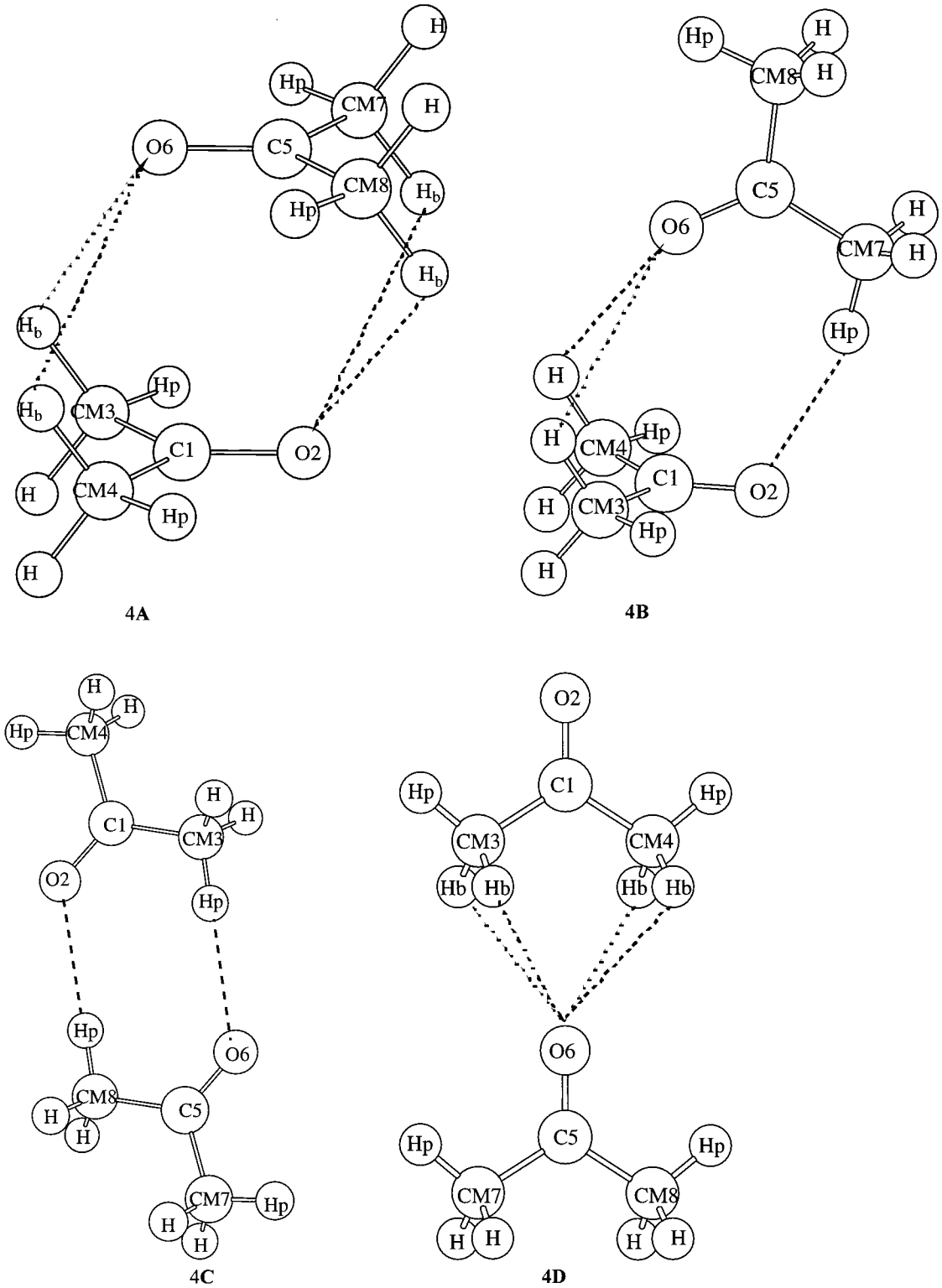

Figure 4. Configurations corresponding to stationary points of the fitted potential surface (values of geometric parameters and interaction energies are listed in Table 3).

4B and its geometric parameters are listed in Table 3 under the heading Fit TS1. Frurip et al.[11] found no stationary point of this kind.

The stationary point of next lowest energy of the fitted potential is a minimum. It has an energy of −2.32 kcal/mol, and the corresponding configuration, which has two hydrogen bonds, is described in the Fit TS2 column of Table 3 and is shown in Figure 4C. Several circumstances suggest that the dimer really has a transition state rather than a stable conformer with this kind of configuration. First, the *ai* intermolecular dimer energy does have a transition state nearby (Inter. TS2 column in Table 3). Second, the minimum is very shallow, as is shown by the very low value of its lowest intermolecular vibrational frequency, 4.9 cm^{-1}, and by the existence of atransition state with an interaction energy only 0.03 kcal/mol higher very nearby (its C1−C5 distance differs by only 0.073 Å from that obtaining at the minimum). Hence, this minimum has been attributed to an artificial minimum produced by the

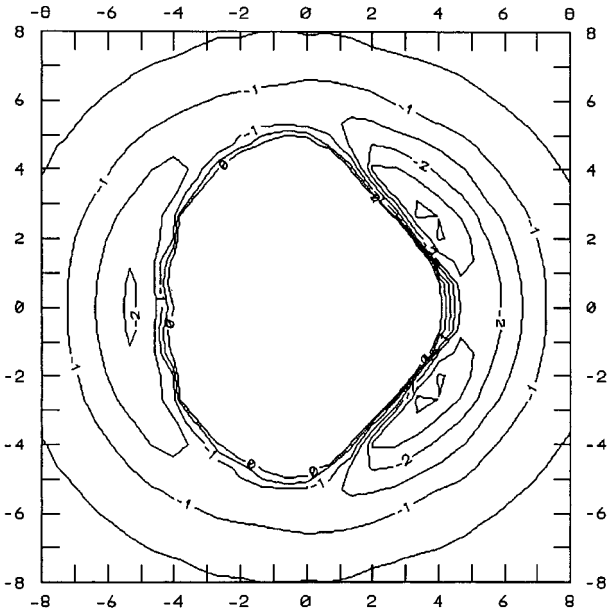

Figure 5. Isoenergetic contour map for acetone−acetone interaction in the CM·C(O)·CM plane of the base monomer.

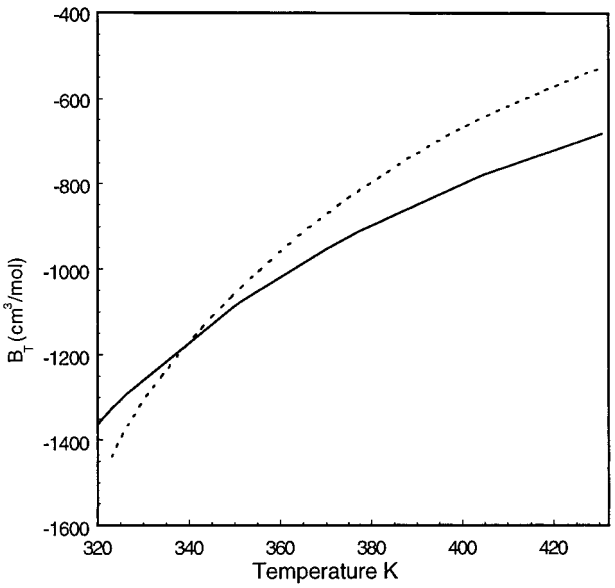

Figure 6. Temperature dependence of the second virial coefficient, as given by experimental data[28] (.....) and by the fitted potential function (—).

function in a flat region of the surface. In other words, it is considered that in the place of this region where such a transition state would be located, there is a very shallow potential well with energies that can be included in the error range of the method. Taking into account the well energies except at very low temperatures, such a shallow minimum will behave effectively as a transition state in simulation studies. A similar configuration, with a C1−C5 distance of 4.65 Å and an interaction energy of −1.65 kcal/mol, was the lowest-energy conformer found by Frurip et al.[11]

Finally, the fitted potential also has a transition state corresponding to the head-to-tail configuration shown in Figure 4D (see also Table 3, Fit TS3 column). Like the absolute minimum, this configuration has four hydrogen bonds, but they are very weak because all four involve the same oxygen atom and the energy is −2.21 kcal/mol.

The full optimized geometries and vibrational frequencies of the *ai* TS1 and TS2 stationary points can be obtained from the authors upon request.

3.4. Isoenergetic Contours and Second Virial Coefficient. To check that the fitted potential behaved reasonably in regions for which no *ai* data had been calculated, we examined isoenergetic contour maps and second virial coefficient, both generated using the program MOLSIM.[27] Figure 5 shows the map obtained in the CM·C(O)·CM plane of the base monomer, which is located with its central carbon atom at the origin and its C═O bond pointing along the negative *x* axis (the energy of each point in the map is the minimum of the potential when the other monomer is allowed to rotate whereas its central carbon remains fixed at that point). The contours are satisfactorily smooth, with no untoward irregularities, and are properly symmetric about the C═O bond. The interaction between the two monomers is basically isotropic at long range, but anisotropy at shorter distances gives rise to stationary points. The two minima with energies rather lower than −3.0 kcal/mol near the oxygen atom, ∼2.5 Å on either side of the axis, may represent configurations similar to that of Figure 4B, whereas the minimum with an energy of about −2.1 kcal/mol that lies on the axis near the methyl groups probably represents the configuration of Figure 4D.

Figure 6 shows the temperature dependence of the second virial coefficient as calculated by MOLSIM[27] using the fitted potential function and as obtained from experimental data. The theoretical value is ∼7.5% less negative than the experimental value at 320 K and ∼29% more negative at 420 K, and the two curves cross each other at ∼340 K (the slope of the theoretical curve is less than that of the experimental curve at all temperatures in this range). At low temperatures, the second virial coefficient depends chiefly on the low energy regions of the interaction potential, suggesting that the potential wells of the fitted function are shallower than those of the real interaction (which is in keeping with the *ai* data to which the function was fitted and which had been obtained with the intramolecular geometry held constant, in view of the discussion about Figure 3). However, using the value of 7.5% for the error at 320 K, the error ΔE in these wells may be roughly estimated from the equation[29] $\ln 0.925 = \Delta E/RT$ as only ∼0.05 kcal/mol. At higher temperatures, at which higher-energy regions of the potential are involved (so that the width and profile of the potential wells become as important as their depth), the fact that the theoretical second virial coefficient is more negative than the experimental values shows that the fitted potential overestimates intermolecular attraction and has wells that are wider than they should be. The error ΔE estimated using the same equation is ∼0.28 kcal/mol, which is greater than for lower-energy regions (as expected) but is still acceptable. The good results at temperatures of ∼340 K might be due to the compensation of the aforementioned effects.

3.5. Simulation of Liquid Acetone. To test the quality of the potential previously calculated, a MC simulation was performed with the MOLSIM[27] package. We used 512 acetone molecules enclosed in a cubic box of length 39.69 Å; periodic boundary conditions were used together with a spherical cutoff of 19.25 Å. The simulation was carried out in the NVT ensemble at a temperature of 298.15 K. In each particle transfer step, a randomly selected molecule was translated in a random direction by a random distance that was no more than 0.2 Å. This displacement was followed by a random rotation of the molecule of <20° around a random axis. Initially the system was equilibrated for 3000*N* particle transfer steps. The calculated properties were then averaged on 1000 independent configurations separated by 10*N* moves each.

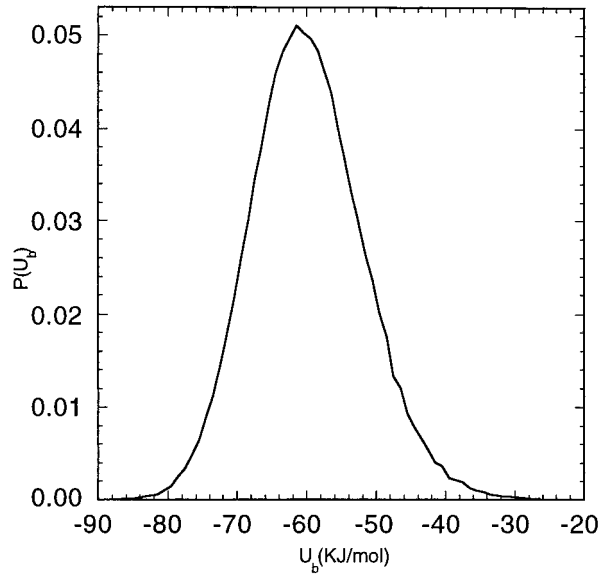

Figure 7. Energy distribution of the acetone molecules.

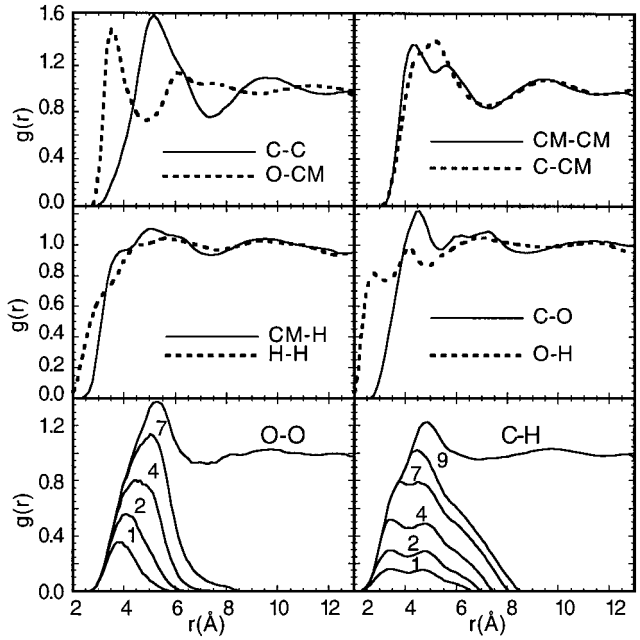

Figure 8. Atom−atom pair correlation functions of acetone. For $g_{C-H}(r)$ and $g_{O-O}(r)$ the contribution of the *n* (number above the curve) nearest neighbors is shown.

The resulting potential energy of the simulated system, −29.92 kJ/mol, is similar to results obtained with empirical potentials[7,25] (we did not found any experimental value for this magnitude). Figure 7 shows the distribution of the molecular energies; there is a smooth continuum of energies between −85 and −35 kJ/mol.

Atomic Radial Distribution Functions and Cosine Distributions. The partial pair correlation functions calculated from the MC simulation are presented in Figure 8. For pairs C−H and O−O, the contributions of the first, second, third, fourth, seventh, and ninth nearest neighbors are also given. These neighbors were classified according to the C−C distance from the C atom of the central molecule. All the distribution functions for pairs of heavy atoms have a double first peak or a shoulder, except for the pairs C−C and O−O. This behavior is similar to the results obtained by Jedlosky et al.[7] in their simulations using a united atom empirical potential. The reasons for these peaks are that, as these authors explain, each molecule

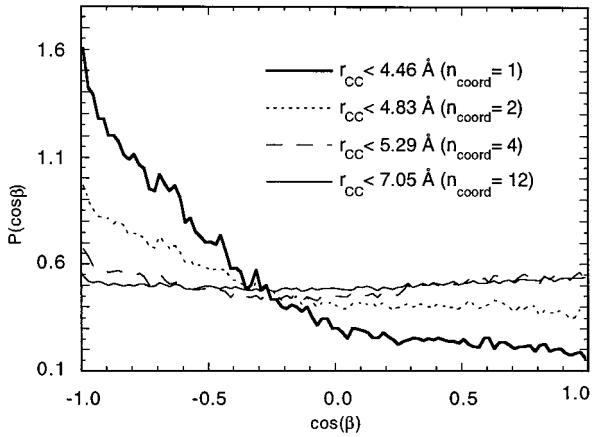

Figure 9. Cosine distribution of the angle β between the C═O bonds of the central and neighbor acetone molecules.

has two CM atoms for the pair correlation functions containing CM atoms, and there are two different C−O separations for the $g_{C-O}(r)$ function. The aforementioned authors obtained a $g_{O-O}(r)$ with two peaks, a small peak at a short distance and another at a much bigger distance. They explain the existence of an antiparallel orientation with the first nearest neighbors different to the other neighbors. We have a correlation function O−O with only one peak using our potential. If the contributions of the neighbors are analyzed, it can be seen that the first nearest neighbors have a peak toward shorter distances than more distant neighbors, but the interval of distances between the peaks is not so long and the peak of the first nearest neighbors is hidden for the contributions of the rest of the first coordination shell.

The functions $g_{H-H}(r)$ and $g_{CM-H}(r)$ show a nearly statistical distribution. This effect is already described by Bertagnolli et al.,[17] and it is due to the numerous and different intermolecular orientations of the hydrogen atoms with respect to each other and to the carbon of the methyl group. The C−H function has only one peak about 4.85 Å. Bertagnolli et al.[17] found the same kind of behavior for the C−H function as for the $g_{H-H}(r)$, but in their C−H distribution, they include the two types of carbon (CM and C) of the acetone molecule. The functions for the nearest neighbors show that the distributions for the first nearest neighbors give two peaks that turn into one peak due to the average with more distant neighbors. We obtained an O−H distribution with a small peak at 2.75 Å (Bertagnolli et al.[17] found this peak at 2.5 Å) and then a bigger one at 4.15 Å; Jedlovszky and Turi[30] observed that one of the pair correlation functions between hydrogen and oxygen in the formic acid showed that behavior.

The center−center pair correlation function of the acetone can be estimated by the C−C pair correlation function. The integration of this function up to its first minima at 7.15 Å yielded a coordination number of 13. This result is consistent with the values of Bertagnolli at al.[17] and Jedlovszky at al.[7] The integration of other partial pair correlation functions give values around the C−C coordination number. Thus, coordination numbers of about 14.5, 13.5, 13, 13, 12, 12, 11, 10, and 3 were obtained for $g_{H-H}(r)$, $g_{CM-H}(r)$, $g_{O-O}(r)$, $g_{CM-CM}(r)$, $g_{C-CM}(r)$, $g_{O-CM}(r)$, $g_{C-H}(r)$, $g_{C-O}(r)$, and $g_{O-H}(r)$, respectively.

The cosine distribution of angle β between the C═O bonds of the central molecule and its neighbors at different distances, each distance corresponding to a coordination number, is shown in Figure 9. For the nearest neighbors the distribution of cos β shows a clear preference for the antiparallel orientation. When the coordination number increases, the distribution tends to a

random behavior very quickly. A Similar tendency is described by Jedlovsky et al.[7] in their results.

4. Conclusions

For satisfactory agreement between experimentally inferred data and *ai* calculations regarding the energy of interaction between the two monomers of the acetone dimer, the *ai* calculations must take electron correlation into account (HF results underestimate the interaction) and the interaction energies must be calculated by the counterpoise method to avoid basis set superposition error.

The analytical potential function fitted to a sample of *ai* energies calculated as already specified (those of 327 configurations with the same intramolecular monomer geometry) was satisfactory from a statistical point of view.

The global minimum of the fitted function has an energy of −4.83 kcal/mol and a C_{2h} geometry with four hydrogen bonds. Calculations on a nearby configuration (the ai sample configuration of least interaction energy) suggest that, due to the shortening of the hydrogen bonds, this value would be lowered by ∼0.35 kcal/mol if the intramolecular geometry of the monomers were optimized.

The dimer has three major transition states, whose energies depend on the number of their hydrogen bonds, on whether these bonds are coplanar, and on the number of oxygen atoms involved in these bonds. The isoenergetic contour map exhibits no irregularities that might throw doubt on the validity of the fitted potential.

Comparison of experimental values for the second virial coefficient in the temperature range 320−420 K with those calculated from the fitted potential function supports the conclusion that the fitted function represents the depth of potential wells quite accurately but overestimates their width.

The liquid acetone properties obtained with our potential agree to a fairly high degree with experimental data and empirical potentials. There are only small differences corcerning other data for the potential energy and the value of the coordination number for the first coordination shell. The potential shows a tendency to antiparallel orientation between the central molecule and the first neighbors, as Jedlovszky et al.[7] suggest, and against the results obtained by Bertanolli et al.[17]

Acknowledgment. We are pleased to acknowledge financial support of this research from Xunta de Galicia. J.M.H. thanks the Segundo Gil Davila Foundation for a grant. Time allocation for calculations was generously provided by the Centro de Supercomputación de Galicia (CESGA).

References and Notes

(1) Allen, M. P.; Tildesley, D. J. *Computer Simulation of Liquids*; Clarendon: Oxford, 1987.
(2) Anwander, E. H. S.; Probst, M. M.; Rode, M. R. *Chem. Phys.* **1992**, *166*, 341.
(3) Michopoulos, Y.; Botschwina, P.; Rode, M. R. *Z. Naturforsch* **1990**, *46a*, 32.
(4) Nakanishi, N.; Ikari, K.; Okazaki, S.; Touhara, H. *J. Chem. Phys.* **1984**, *80*, 1656.
(5) Okazaki, S.; Nakanishi, N.; Touhara, H. *J. Chem. Phys.* **1983**, *78*, 454.
(6) Vizoso, S.; Heinzle, M. G.; Rode B. M. *J. Chem. Soc., Faraday Trans.* **1994**, *90*, 2337.
(7) Jedlovszky, P.; Pálinkás, G. *Mol. Phys.* **1995**, *84*, 217.
(8) Evans, G. J.; Evans, M. W. *J. Chem. Soc., Faraday Trans. 2* **1983**, *79*, 153.
(9) Bródka, A.; Zerda, T. W. *J. Chem. Phys.* **1996**, *104*, 6313.
(10) Knözinger, E.; Wittenbeck, R. *J. Mol. Spectrosc.* **1984**, *105*, 314.
(11) Frurip, D. J.; Curtiss, L. A.; Blander, M. *J. Phys. Chem.* **1978**, *82*, 2555.
(12) Swaminathan, S.; Whitehead, R. J.; Guth, E.; Beveridge, D. L. *J. Am. Chem. Soc.* **1977**, *99*, 7817.
(13) *Gaussian 94, Revision C.3* Frisch, M. J.; Trucks, G. W.; Schlegel, H. B.; Gill, P. M. W.; Johnson, N. G.; Robb, M. A.; Cheeseman, J. R.; Keith, T.; Petersson, G. A.; Montgomery, J. A.; Raghavachari, K.; Al-Laham, M. A.; Zakrzewski, V. G.; Ortiz, J. V.; Foresman, J. B.; Cioslowski, J.; Stefanov, B. B.; Nanayakkara, A.; Challacombe, M.; Peng, C. Y.; Ayala, P. Y.; Chen, W.; Wong, M. W.; Andres, V; Replogle, E. S.; Gomperts, R.; Martin, R. L.; Fox, D. J.; Binkley, J. S.; Defrees, D. J.; Baker, J.; Stewart, V.; Head-Gordon, M.; Gonzalez, C.; Pople, J. A. Gaussian: Pittsburgh, PA, 1995.
(14) Frisch, M.; Del Bene, J.; Binkley, J.; Schaefer, V., III *J. Chem. Phys.* **1986**, *84*, 2279.
(15) Iijima, T. *Bull. Chem. Soc. Jpn.* **1972**, *45*, 3526.
(16) Bertagnolli, H.; Hoffmann, M. *Z. Phys. Chem. Neue Folge* **1988**, *159*, 185.
(17) Bertagnolli, H.; Hoffmann, M. *Z. Phys. Chem. Neue Folge* **1989**, *165*, 165.
(18) Peter, R.; Dreizler, H. *Z. Naturforsch.* **1965**, *20a*, 301.
(19) Dunning, T. H., Jr.; Hay, P. J. In *Modern Theoretical Chemistry*; Schaefer III, H. F., Ed.; Plenum: New York, 1976.
(20) Gordon, M. S. *Chem. Phys. Lett.* **1980**, *76*, 163.
(21) Boys, S. F.; Bernardi, F. *Mol. Phys.* **1970**, *19*, 553.
(22) Szalewicz, K.; Cole, S.; Kolos, W.; Bartlett, R. *J. Chem. Phys.* **1988**, *89*, 3662.
(23) Marquardt, D. *SIAM J. Appl. Math.* **1963**, *11*, 431.
(24) Wee, S. S.; Kim, S.; Jhon, M. S.; Scheraga, H. A. *J. Phys. Chem.* **1990**, *94*, 1656.
(25) Ferrario, M.; Haughney, M.; McDonald, I. R.; Klein, M. L. *J. Chem. Phys.* **1990**, *93*, 5156.
(26) Stone, A. J.; Popelier, P. A. L.; Wales, D. J. *Orient: A program for studying interactions between molecules. Version 3.1.1*; University of Cambridge: Cambridge, 1995.
(27) Linse, P.; Wallqvist, A. *MOLSIM 1.2*, Lund University: Lund, Sweden 1991.
(28) Bottomley, G. A.; Spurling, T. H. *Aust. J. Chem.* **1967**, *20*, 1789.
(29) Karlström, G.; Linse, P.; Wallqvist, A.; Jönsson, B. *J. Am. Chem. Soc.* **1983**, *105*, 3777.
(30) Jedlovszky, P.; Turi, L. *J. Phys. Chem. B* **1997**, *101*, 5429.